New Journal of Physics
The open-access journal for physics

Atomic wave packets in amplitude-modulated vertical optical lattices

A Alberti[1,2], G Ferrari[1,3], V V Ivanov[4], M L Chiofalo[5] and G M Tino[1,6]

[1] Dipartimento di Dipartimento di Fisica e Astronomia and LENS-Università di Firenze, INFN-Sezione di Firenze, via Sansone 1, 50019 Sesto Fiorentino, Italy
[2] Institut für Angewandte Physik der Universität Bonn, Wegelerstrasse 8, 53115 Bonn, Germany
[3] Istituto Nazionale di Ottica (INO)-CNR, Largo Fermi 6, 50125 Florence, Italy
[4] Department of Physics, University of Washington, 3910 15th Avenue NE, Seattle, WA 98195-1560, USA
[5] Department of Mathematics and INFN, University of Pisa, Largo B. Pontecorvo 5, 56127 Pisa, Italy
E-mail: guglielmo.tino@fi.infn.it

New Journal of Physics **12** (2010) 065037 (14pp)
Received 10 February 2010
Published 28 June 2010
Online at http://www.njp.org/
doi:10.1088/1367-2630/12/6/065037

Abstract. We report on the realization of dynamical control of transport for ultra-cold ^{88}Sr atoms loaded in an accelerated amplitude-modulated one-dimensional (1D) optical lattice. We show that the behavior of the dynamical system can be viewed as if traveling wave packets were moving in a static lattice whose energy dispersion can be tailored at will in width, amplitude and phase. One basic control operation is a reversible switch between Wannier–Stark localization and driven transport based on coherent tunneling. Performing modulation sequences of this operation within a Loschmidt-echo scheme, we are able to reverse the atomic group velocities at once. We then apply the technique to demonstrate a novel mirror for matter waves working independently of the momentum state. We finally discuss advantages of amplitude over previously reported phase modulation techniques for applications in force measurements at micrometric scales.

[6] Author to whom any correspondence should be addressed.

Contents

1. Introduction

Atoms trapped in optical lattice potentials in the absence of defects and phonon excitations are extremely versatile systems for quantum applications [1], including transport [2, 3] and realization of strongly correlated phases [4–7]. In addition, control of atomic interactions may keep the dynamics coherent over seconds [8, 9] and has led to atomic optical clocks with extraordinary performances [10, 11], determination of forces with micrometer resolution [12–19] and quantum information processing [20–24].

Tailoring and control of the coherent transport behavior is an essential tool for these applications [25]. Dynamical mechanisms, such as phase or amplitude lattice modulations, can be designed to drive transport behavior over desired time and length scales. Phase modulation, obtained by a periodic spatial displacement of the optical lattice, has been exploited to investigate quantum chaos [26] and, under the effect of constant forces, to observe Wannier–Stark resonances [27], photon-assisted resonant tunneling [18, 28], quantum transport over macroscopic distances [29] and dynamical control of Mott insulator transitions [30]. Amplitude modulation has been used so far as a spectroscopic tool for interband excitations [31], to induce parametric heating [32, 33] and to characterize the Mott insulator regime [34]. Analogous techniques are produced by acoustoelectric means in semiconductor nanostructures in the form of surface acoustic waves, aimed at making single-photon high-frequency sources [35, 36] and drive delocalization [37], but in this case the relevant spatial scale is much longer than the underlying static lattice.

In this paper, we report on the dynamical control of coherent transport of atomic wave packets, which is realized through amplitude modulation of vertical optical lattices. While extensive theoretical studies on phase modulation of optical lattices are available [38–40], the physics underlying the control of transport through amplitude modulation is to our knowledge largely unexplored, together with its experimental realizations. We show that amplitude modulation brings two main differences over phase modulation which can be useful for applications. Amplitude modulation is characterized by a linear dependence of the tunneling rates on the amplitude of the external driving, which allows one to operate the wanted effects over a wide range of the governing parameters, while the phase modulation is characterized by a nonlinear response, giving rise to dynamical localization [41]. In addition, amplitude

modulation allows the implementation of the method much closer to a reflective substrate, which turns out to be very useful for precision measurements at micrometric distances.

We show that the dynamical system behavior can be viewed as if traveling wave packets were moving in a static lattice whose energy dispersion can be tailored at will in width, amplitude and phase. Using this simplified view as a guide for the experiment, we demonstrate basic control operations, such as reversible switch between Wannier–Stark localization and driven transport based on coherent tunneling. Applications of these techniques bring some advantages in the design of tools for force measurements at micrometric scales and matter-wave transport. In fact, by performing a two-burst modulation sequence within a Loschmidt-echo scheme [42, 43], we reverse the atomic group velocities at once and demonstrate a novel mirror for matter waves working independently of the momentum state.

The paper is organized as follows. We illustrate the concepts underlying amplitude modulation and the theoretical characterization of our system in section 2, where it is shown how the effective energy dispersion can be tailored. The experimental method and setup are described in section 3. The results are illustrated in section 4, where we characterize the resonant tunneling and demonstrate new tools for quantum transport control, namely the realization of Loschmidt echoes and of a novel kind of atom mirror. We conclude this section by testing the present scheme on a 0.5 ppm measurement of the local acceleration of gravity. We discuss the advantages of using amplitude over phase modulation at each step, and draw our concluding remarks in section 5.

2. The model: tailoring the energy dispersion

We consider a one-dimensional (1D) optical lattice originated by the interference pattern of two vertical counter-propagating laser beams with wavelength λ_L, so that atoms effectively see a periodic potential with a period $d = \lambda_L/2$ and a depth dictated by the laser intensity, which we modulate in time. Our system is then described by the 1D time-dependent single-particle Hamiltonian

$$\mathcal{H}(z, p, t) = \frac{p^2}{2m} - U(z)\,[1 + \alpha f(t)] + mgz, \tag{1}$$

where $U(z) = U_0 \cos(2k_L z)/2$ and

$$f(t) \equiv \sin\left[\omega_M (t - t_0) - \phi\right]. \tag{2}$$

As sketched in figure 1(a), U_0 is the lattice depth, $k_L = 2\pi/\lambda_L$ is the laser wave vector, m is the atomic mass and g is the gravity acceleration along the lattice direction. The modulation is characterized by its amplitude $0 < \alpha < 1$ expressed in units of U_0, frequency $\omega_M = \ell\omega_B$ that is the ℓth harmonic of the Bloch frequency $\omega_B = mgd/\hbar$, time t_0 when the modulation is switched on with initial phase ϕ. We explicitly leave the possibility of independently play t_0 and ϕ in view of applying repeated sequences of amplitude modulation bursts.

When the modulation is off ($\alpha = 0$), it is well known that the resulting static Hamiltonian $\mathcal{H}_0$ is diagonalized by the so-called Wannier–Stark states $|n\rangle$ centered on the nth lattice site and separated in energy by quanta of $\hbar\omega_B$ [44]. These are in turn built up from the Wannier functions $|w(m)\rangle$ of the non-tilted ($g = 0$) lattice centered at the mth site.

From now on we consider working in a deep lattice with $U_0 \gg E_R$ on the scale of the recoil energy $E_R = h^2/(2m\lambda_L^2)$. Under these conditions, the energy gap E_G is sufficiently large on the scale of mgz and $\hbar\omega_M$, so that the band-to-band coupling due to the exchange of ω_M quanta

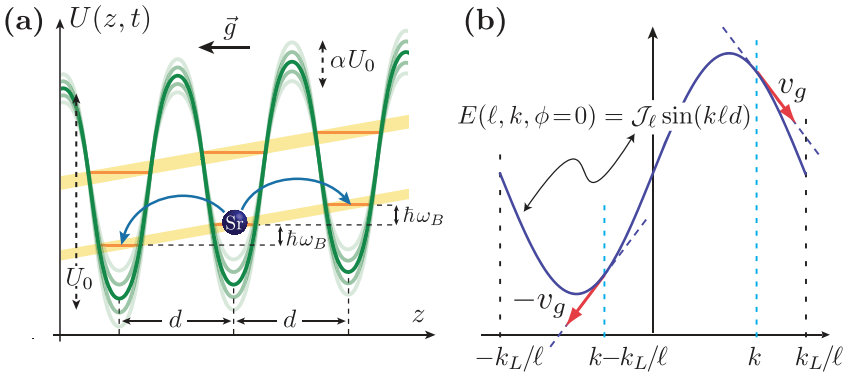

Figure 1. Sketch of the transport mechanism in the amplitude-modulated lattice. (a) In the real space: Wannier–Stark localized states populate the tilted lattice of energy potential $U(z,t)$. In the absence of amplitude modulation, $\alpha = 0$, the inter-site tunneling is suppressed. Coherent tunneling between sites ℓd apart is enabled when the amplitude modulation is switched on at $\omega_M = \ell\omega_B$. (b) In the momentum space, wave packets behave as if they were moving in an effective sinusoidal energy band, whose width, periodicity and phase can be tailored by means of the amplitude-modulation parameters. Because of the sinusoidal shape, the group velocity v_g is reversed when $k \to k - k_L/\ell$. Only the unit cell $[-2k_L/\ell, 2k_L/\ell]$ of the effective and periodic energy band of 6 is shown.

is negligible. In this regime where also the Landau–Zener tunneling is suppressed, we can safely restrict ourselves to a single-band description with no interband transitions. Wave packet tunneling is thus frozen due to Wannier–Stark localization and Bloch oscillations set in, where the quasi-momentum spans the Brillouin zone $[-k_L, k_L]$ with Bloch period $\tau_B = 2\pi/\omega_B$ [2, 3].

In order to obtain the picture of the system behavior when the modulation is switched on at frequency $\ell\omega_B$, we first observe that in the basis set of the Wannier–Stark states $|n\rangle$ the Hamiltonian (1) reads

$$\mathcal{H} = \sum_{n=-\infty}^{\infty} n\hbar\omega_B |n\rangle\langle n| - \frac{\alpha U_0}{2}\sin(\omega_M(t-t_0)-\phi) \sum_{\substack{\ell>0 \\ n=-\infty}}^{\infty} (\mathcal{C}_\ell |n+\ell\rangle\langle n| + \text{h.c.}), \tag{3}$$

where $\mathcal{C}_\ell \equiv \langle n+\ell|\cos(2k_L z)|n\rangle$ and due to translational symmetry we have dropped the diagonal term $-(\alpha\, U_0/2)\,\mathcal{C}_0 \sin(\omega_M(t-t_0)-\phi)|n\rangle\langle n|$.

We then use the unitary transformation $\mathcal{U} = \exp\left(-\mathrm{i}\sum_{n=-\infty}^{\infty}(n/\ell)\omega_M(t-t_0)|n\rangle\langle n|\right)$ to move to the rotating frame where the secular approximation is applied discarding the off-resonant terms with respect to the resonance at $\omega_M = \ell\omega_B$. In particular, the interband transitions can safely be neglected because they are far from resonance under our experimental conditions. In this rotating frame, the Hamiltonian of (1) is simplified into $\mathcal{H}' = \mathcal{U}^\dagger\mathcal{H}\mathcal{U} - \mathrm{i}\hbar\,\mathcal{U}^\dagger\,\mathrm{d}\mathcal{U}/\mathrm{d}t$, that is

$$\mathcal{H}' = \sum_{n=-\infty}^{\infty}\left[\mathrm{i}\left(\frac{\mathcal{J}_\ell}{2}\right)\mathrm{e}^{\mathrm{i}\phi}|n+\ell\rangle\langle n| + \text{h.c.}\right] \tag{4}$$

with tunneling rates

$$\mathcal{J}_\ell = -\frac{\alpha U_0}{2}\langle n+\ell|\cos(2k_{\mathrm{L}}x)|n\rangle. \tag{5}$$

The Hamiltonian (4) predicts that coherent resonant tunneling can be established between sites spatially separated by ℓd [18], as sketched in figure 1(a).

In real space, this site-to-site tunneling can be viewed as a two-photon stimulated Raman process where the amplitude (phase) modulation brings about in-(out-of-)phase sidebands of the original lattice [31]. In momentum space the atomic wave packets behave as if they were moving with an effective energy dispersion

$$E(\ell, k, \phi) = \mathcal{J}_\ell \sin(k\ell d - \phi), \tag{6}$$

as depicted in figure 1(b), where each of the three parameters $\mathcal{J}_\ell$, ℓ and ϕ can be accurately tuned, by acting, respectively, on the amplitude of modulation α, on the choice of the modulation harmonic of ω_{B} and on the initial phase at which the modulation is started. This tunable sinusoidal energy profile has deep consequences for the transport behavior, as proved by the experimental results in the following sections. Firstly, the profile is periodic within the Brillouin zone with a period $2k_{\mathrm{L}}/\ell$. This periodicity physically results from the resonant tunneling which selectively couples sites that are separated by ℓ lattice periods d. Secondly, both ϕ and the energy bandwidth $\mathcal{J}_\ell$ can be tuned, the latter being linear in the full range of modulation amplitudes $0 < \alpha < 1$. Finally, the group velocity

$$v_{\mathrm{g}}(\ell, k, \phi) = \frac{\partial E(\ell, k, \phi)}{\partial(\hbar k)} = \frac{\ell d}{\hbar}\mathcal{J}_\ell \cos[k\ell d - \phi] \tag{7}$$

reverses its sign whenever $k \to k + (2n+1)\, k_{\mathrm{L}}/\ell$ for any integer n, as shown in figure 1(b). This recalls the Loschmidt-echo scheme in [42, 43], where it is shown that the wave vector mapping is equivalent to reversing the band curvature $\mathcal{J}_\ell \to -\mathcal{J}_\ell$. We thus proceed to illustrate the experiment where this basic operation of reversing the group velocities is performed and exploited for quantum transport control and for precision measurements.

3. Experimental apparatus

The source of ultra-cold atoms has been described elsewhere [16], therefore we only provide essential information here. We start by trapping and cooling about 2×10^7 ^{88}Sr atoms at 3 mK in a magneto-optical trap (MOT) operating on the $^1\mathrm{S}_0 - ^1\mathrm{P}_1$ resonance transition at 461 nm. The temperature is further reduced by a second cooling stage in a red MOT operating on the $^1\mathrm{S}_0 - ^3\mathrm{P}_1$ intercombination transition at 689 nm. Finally, we obtain $\sim 1 \times 10^6$ atoms at 1 μK. We load the atoms in the optical lattice, which is switched on adiabatically in 80 μs. The atomic sample arranges itself in a disc-shaped geometry with a vertical rms size of about $\sigma_0 = 30\,\mu$m. Atomic interactions here are negligible because of the tiny scattering length in the ground state $a = -1.4\, a_0$ [45]. The lattice potential is originated by a single-mode frequency-doubled Nd : YVO_4 laser ($\lambda_{\mathrm{L}} = 532$ nm) delivering up to 1 W on the atoms with a beam waist of 250 μm. The beam is vertically aligned and retro-reflected by a mirror. The resulting Bloch frequency is $\omega_{\mathrm{B}} = 2\pi \times 574.3\,\mathrm{s}^{-1}$. The corresponding photon recoil energy is $E_{\mathrm{R}} = 2\pi \times 8000\,\mathrm{s}^{-1}$, and the lattice depth of the static lattice is fixed in a range from $5E_{\mathrm{R}}$ to $20E_{\mathrm{R}}$, when the energy gap at k_{L} is $E_{\mathrm{G}} \gtrsim 3E_{\mathrm{R}} \gg \hbar\omega_{\mathrm{B}}$ and the bandwidth is always smaller than $10^{-1}E_{\mathrm{G}}$. Given these conditions, Landau–Zener tunneling is negligible. By controlling the radio-frequency power of

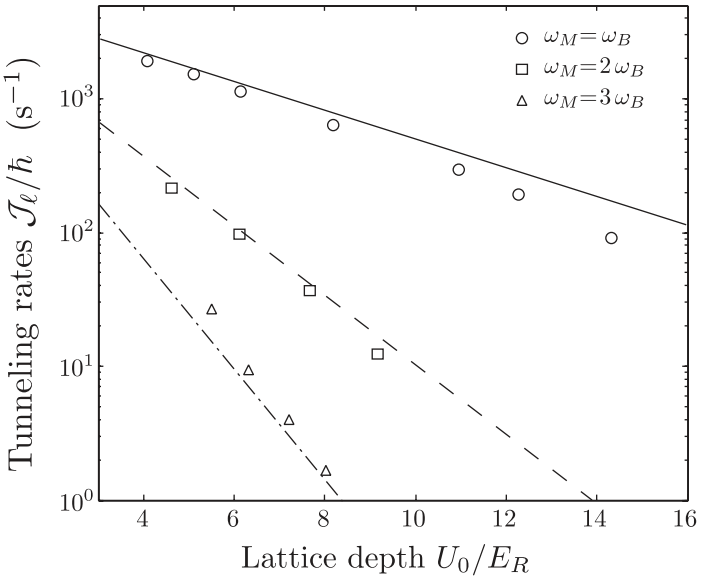

Figure 2. Tunneling rates of the resonantly driven transport. The points with different symbols correspond to the measured tunneling rates for the first three harmonics of modulation $\ell = 1, 2, 3$ as a function of the lattice depth U_0/E_R (see legend). By relying on the linearity of the tunneling as a function of the modulation amplitude α, the data have been normalized so that $\alpha U_0 = 2E_R$. The lines correspond to the computed theoretical values (see text). The error bars are in the size of the symbols.

an acousto-optical modulator, we stabilize and modulate the laser intensity in order to reproduce the time-dependent Hamiltonian in (1). The readout is performed by measuring *in situ* the spatial atomic distribution using resonant absorption imaging.

4. The results

4.1. Resonant tunneling in amplitude-modulated optical lattices

To characterize the tunneling rates $\mathcal{J}_\ell$ we proceed as follows. The atoms are initially localized to single lattice sites, their quasi-momenta being spread over the whole Brillouin zone. In fact, the de Broglie wavelength results $\lambda_{\rm dB} \sim 200\,{\rm nm} < d$ at temperature $T \sim 1\,\mu$K. Applying the amplitude modulation for a given time results in a spatial broadening of the atomic wave packets. The speed of this broadening corresponds to the average over k of the group velocities $\langle v_{\rm g}^2\rangle^{1/2} = \ell d\mathcal{J}_\ell/(\sqrt{2}\hbar)$ [39], which, thus, provides a measurement of $\mathcal{J}_\ell$. We measure the speed of broadening by recording the spatial size of the atomic cloud at different times of modulation and fitting the resulting curve by a linear expansion [18]. By varying the modulation amplitude $0 < \alpha < 1$, we find that the $\mathcal{J}_\ell$ depend linearly on it. This is a unique feature of amplitude modulation, which provides a clean tunability of the $\mathcal{J}_\ell$ across a wide range. This is shown in figure 2, where the measured $\mathcal{J}_\ell$ values, represented by symbols, are shown together with the numerical values, represented by lines, while varying the lattice depth U_0. The numerical curves are computed by using expression (5) and an analytical expression of the Wannier–Stark states

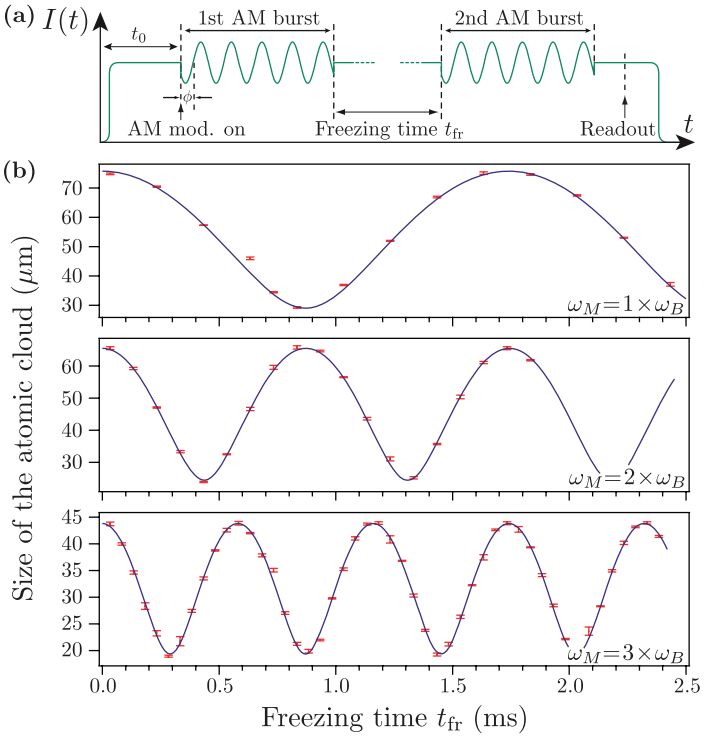

Figure 3. Realization of Loschmidt echoes (a) The applied sequence: two identical amplitude-modulation (AM) bursts of the optical lattice intensity $I(t)$ at $\ell\omega_B$ enable the resonant tunneling, which couples lattice sites separated by ℓd. The bursts are separated by a *freezing time* t_{fr}, during which the tunneling is disabled and Bloch oscillations of the quasi-momentum set in. (b) The corresponding cloud's rms size versus t_{fr} has periodicity $2\pi/(\ell\omega_B)$. From top to bottom, the amplitude modulation at $\omega_M = \ell\omega_B$ induces resonant coupling with up to $\ell = 3$ neighboring sites. Inversion of the group velocities v_g occurs at the minima of the rms size.

$|n\rangle$, which is valid in the regime of deep lattices [44]. The agreement is excellent in all three cases $\ell = 1, 2, 3$ of harmonic modulation.

4.2. Loschmidt echoes

In order to demonstrate the reversal of the group velocities, we employ the sequence in figure 3(a), using a Loschmidt-echo scheme analogous to the more familiar spin echo in other systems [42, 43]. Two identical amplitude-modulation bursts characterized by the same amplitude, phase and by the frequency $\ell\omega_B$ are applied lasting about 500 ms each, which correspond to 287 Bloch periods τ_B, where τ_B has been preliminarily measured with 1 ppm sensitivity [18]. For each case $\ell = 1, 2, 3$, we choose U_0 and α in a way to keep comparable tunneling rates and stay within the same regime of operation. It turns out that, while we decrease U_0 through the values $U_0 = 11.2E_R, 6.6E_R, 6.3E_R$, we have to increase α through the values $\alpha = 0.23, 0.47, 0.84$.

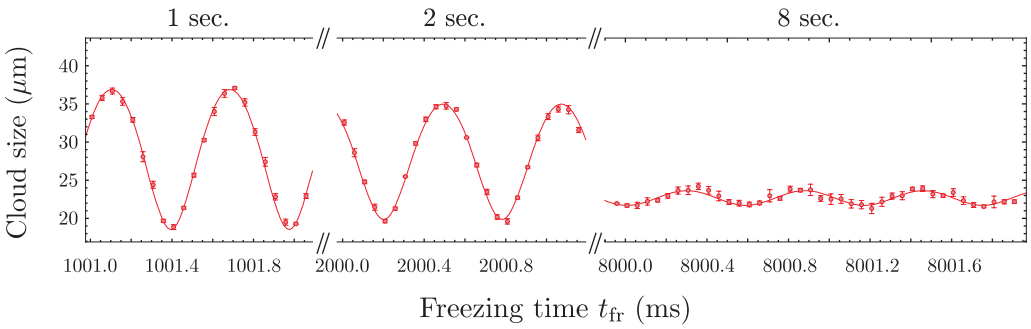

Figure 4. Loschmidt echoes persisting over a long period. The data points report the full data series corresponding to the case of $\omega_M = 3\omega_B$ reported in figure 3. The damping time is estimated to be of the order of 4 s.

The two bursts serve to enable the coherent tunneling and are separated by a variable *freezing time* t_{fr} during which the amplitude modulation is off, $\alpha = 0$, and the resonant tunneling is disabled. During the *freezing time*, the quasi-momentum increases linearly in time performing Bloch oscillations within the Brillouin zone with period τ_B. This corresponds, in other terms, to a phase imprinting created by the linear gravity potential on the lattice such that neighboring sites acquire a $\omega_B t_{fr}$ phase difference. The group velocity $v_g(\ell, k, \phi)$ during the second burst depends on the group velocity during the first burst and on the phase imprinting during the *freezing time*. The overall cloud's expansion or contraction during the second burst is related to the comparison of the group velocities before and after the *freezing time*, whether they are aligned or anti-aligned as shown in figure 1(b). By varying t_{fr}, the two situations alternate periodically with period $\tau_\ell \equiv \tau_B/\ell$, proving the ℓ-fold periodicity of the effective energy band within the Brillouin zone. Figure 3(b) shows that this is indeed the case, resulting in a periodic signal with period τ_ℓ. The group velocities $v_g(\ell, k, \phi)$ are fully reversed independently of the k values at each $\tau_\ell/2$, that is at the minima occurring at $t_{fr} = \tau_\ell/2|2n+1|$ (n integer).

The Gaussian convolution of the single-atom response with the initial cloud's distribution suggests that the expression of the rms size is $\sigma(t_{fr}) = \sqrt{\sigma_0^2 + \sigma_1^2 \cos(\pi t_{fr}/\tau_\ell)^2}$, with σ_0 being the initial size. This is reproduced by the solid curves, best agreeing with the measured points. The fit to each data set with different ℓ yields $\tau_\ell = \tau_B/\ell$, and σ_1 turns out to match the broadening that would occur after one single burst twice as long. The oscillations persist over several seconds, indicating a high fidelity in recovering the quantum state after v_g reversal [42, 43]. This is illustrated in figure 4, where the damping time is estimated to be about 4 s.

4.3. A novel kind of atom mirror

The tools developed so far can be used efficiently to realize an atomic mirror for traveling matter waves with defined momentum. In order to observe this effect, we need to prepare the atoms with a momentum dispersion narrower than the Brillouin zone. We accomplish this by increasing $U_0 = 14E_R$ sufficiently to trap a fraction of atoms also in the second band, where the momentum distribution shrinks because here the thermal momentum distribution is steeper. In addition, we purposely favor one of the two directions by letting the atoms freely fall for about 200 μs between the release from the red MOT and the lattice switch on. We can accurately control the value of k within the Brillouin zone by following the Bloch oscillations in the

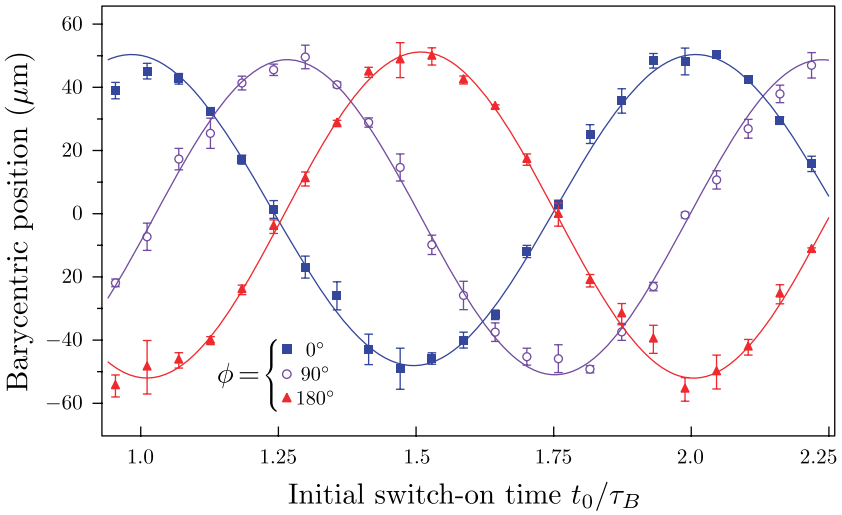

Figure 5. Cloud's barycentric position after a single amplitude-modulation burst versus switch-on time of the amplitude modulation, t_0, at $\omega_M = \omega_B$. Changing the initial hold time t_0 in the static lattice allows one to prepare any initial quasi-momentum within the Brillouin zone. The sinusoidal shape of the data point indicates that the dynamics in the modulated system are described by the effective energy dispersion in equation (6). By varying the modulation phase ϕ of the driving, we shift the sinusoidal energy dispersion by the same amount, e.g. at $\phi = 90^\circ$ from sine to cosine.

static lattice for a time t_0 before activating the amplitude modulation. During the modulation the cloud's position is expected to move with a velocity $v_g(\ell, k, \phi)$ with $k = 2k_L t_0/\tau_B$ modulus the Brillouin zone, as it is shown in figure 5. Here, it is also emphasized that besides the width and the periodicity of the dispersion law, we can also tailor its phase at will.

At the flex points of $E(\ell, k, \phi)$, like at $k = 0$ for $\phi = 0$, the motion becomes dispersionless and reaches the largest v_g, and consequently the largest displacement. In this case, figure 6 shows the displacement of the atoms in the second band, which move upwards with a v_g of $0.64\,\mathrm{mm\,s^{-1}}$ when $\alpha = 0.33$ and $\ell = 1$. We track this motion for 500 cycles corresponding to a duration of 870 ms and a displacement of about 0.5 mm. A residual broadening still occurs because of finite spread of the initial momentum distribution, but it is limited to one-tenth of the total displacement. This can largely be reduced by initially preparing a narrower momentum distribution, as with Bragg or Raman velocity selective stages, sympathetic cooling or BECs. In order to reverse the wave-packets' motion, we subsequently apply the scheme of figure 3(a) by choosing $t_{fr} = \tau_B/2$. During the second burst, the atoms move downwards with the same speed but opposite direction. As expected, the atom mirror reverses the direction of motion as well as the broadening of the atomic cloud, making the traveling wave packets recover their initial size at the echo time of 500 cycles when the duration of the second burst equals the duration of the first one, analogously to the Loschmidt echoes shown in figure 3.

4.4. Gravity measurements

The control of transport obtained here with resonantly driven optical lattices can be exploited to determine with high-precision the local forces applied to the atoms. In addition, since

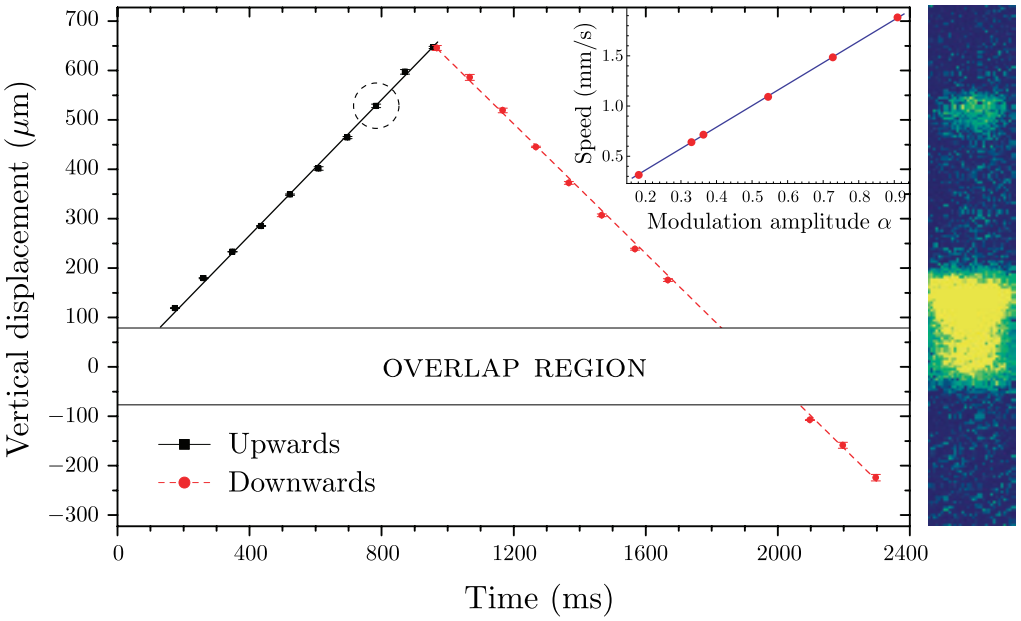

Figure 6. Atom mirror for traveling matter waves. Atoms loaded in the second band have sub-recoil momentum dispersion. Wave packets with initial $k = 0$ travel upwards with minor dispersion (solid line). After reversing the group velocity v_g, atoms move downwards with opposite speed (dashed line). Inset: linearity of the tunneling versus the modulation amplitude α. Right panel: 2D density profile of the cloud corresponding to the data point, circled in figure, at $t = 783$ ms. Because the atoms in the second band have a higher v_g, the two clouds separate from each other away from the origin.

measurements here occur with atoms trapped in confined geometries, this type of technique is well suited in applications where high spatial resolution is required. In this regard, we expect to reach micrometer spatial resolutions by properly reducing the initial size of the atomic sample.

As we have already demonstrated using phase modulation techniques [18], we can provide high-precision determination of the Bloch frequency ω_B, which is in turn proportional to the local force experienced by the atoms, by recording the response of the atomic dynamics during a modulation frequency scan around the tunneling resonances centered at $\omega_M = \ell\omega_B$. In [18] we have also demonstrated that the resonance spectra obtained after this measurement are characterized by a width that remains Fourier limited regardless of the harmonic of modulation ℓ. Therefore, by phase modulating the lattice at higher frequency $\ell\omega_B$, we were able to increase the quality factor of the resonances, hence the sensitivity in the determination of the local acceleration of gravity.

The very same effect is observed in the present setting, where we perform an amplitude modulation of the optical lattice potential for a finite time. We obtain resonance spectra that are Fourier limited up to the fifth harmonic of the Bloch frequency, resulting in an improved sensitivity (see below). This is illustrated in figure 7: as expected, the spectrum is shaped like a *sinc* function with a Fourier-limited width, demonstrating that coherent delocalization of the wave packets occurs.

Instead of scanning the tunneling resonances by varying ω_M, it is also possible to exploit the Loschmidt-sequence method described in section 4.2. In this case we can provide a

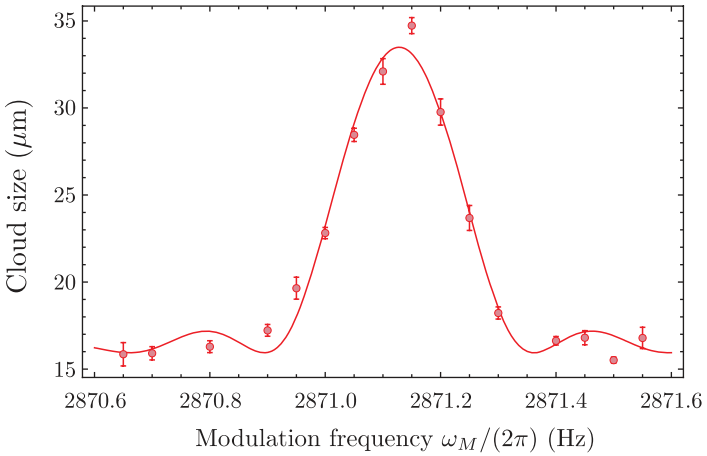

Figure 7. Resonance spectrum after amplitude modulation of the lattice potential. The spectrum is obtained after a modulation time of $t = 5\,\mathrm{s}$ while scanning across the fifth harmonics of the Bloch frequency ω_B. The resonance width is estimated to be 69 mHz close to the Fourier limit of about $1/(\pi t) = 64\,\mathrm{mHz}$, indicating that the corresponding tunneling couples coherently lattice sites that are separated by $5\lambda_\mathrm{L}/2 = 1.3\,\mu\mathrm{m}$. The solid line represents the convolution of the initial spatial size and the broadening that is described by $\mathrm{sinc}(x) = \sin(x)/x$ function with argument $x = \delta t/2$, where $\delta = \omega_\mathrm{M} - 5\,\omega_\mathrm{B}$ is the detuning from resonance and t is the modulation time. From this spectrum, we determine the Bloch frequency ω_B with a statistical uncertainty of about 1 ppm.

measurement of ω_B while working at—or close to—the resonant frequencies $\omega_\mathrm{M} = \ell\omega_\mathrm{B}$. For example, a fit of the data set of figure 3 with $\ell = 3$, obtained following the oscillations for 8 s, yields a measurement of g with relative sensitivity $\Delta g/g = 5 \times 10^{-7}$. The advantage of the Loschmidt-sequence method in which two separated pulses of modulation are used is that the physical signal is integrated during the *freezing time* when the modulation is switched off. This suppresses the atomic losses that originate from the modulation itself. Although the latter occur at a very small rate, they can build up to a significant level on a time scale of several seconds.

A few remarks are now in order, which can be useful to compare these modulation techniques for precise force measurements with other methods, based on the study of Bloch oscillations in static lattices [14, 16, 46]. In the present phase or amplitude modulation techniques, the atomic sample is prepared in a superposition of quasi-momenta states spanning the whole Brillouin zone. This relaxes one important constraint on the temperature, which can be above the recoil energy E_R. In the static-lattice methods, one significant sensitivity requirement is that the temperature is below E_R, in order to initiate the atomic sample in a highly defined quasi-momenta state. In addition, the present techniques directly probe differences of potential energy and thus they can be employed under conditions where strongly curved potentials play a role, as with the Casimir–Polder interaction. This direct sensitivity to potential differences is notably important when compared with the other atomic techniques aiming at exploring inhomogeneous potentials, which are sensitive either to the first [15] or to the second [47] derivative of the external potential, depending on whether one measures Bloch or dipole oscillations in a static lattice, respectively.

We finally remark on an important conceptual advantage of amplitude over phase modulation, regarding the measurement of forces when the atoms are placed close to a macroscopic substrate. In fact, the method based on amplitude modulation can be implemented in the vicinity of a reflective substrate, since an independent control of the two lattice beams is not required. Conversely, in the case of phase modulation, it would be inconvenient to mount a bulky macroscopic substrate on top of a piezoelectric transducer. Besides this intrinsic difference, the use of amplitude modulation has allowed us to observe coherent broadening at higher ℓ values with respect to those previously obtained using phase modulation, and therefore to improve our sensitivity. This is mostly due to purely experimental reasons, since amplitude modulation allows a better control over phase modulation schemes.

5. Conclusions

In conclusion, we have presented a novel method to control the transport of cold atoms in optical lattices. The method is based on an amplitude modulation of the lattice potential on resonance with the Bloch frequency and its harmonics. Under these conditions, the dynamical system can effectively be viewed as a stationary one, where the atomic wave packets move in an effective energy band whose periodicity, width and phase can be tailored at will while acting on the modulation parameters.

Besides the significant interest *per se* of this dynamical energy-band engineering, the flexibility offered by the present method is of great importance for applications. As an example, we have used the basic operation of group velocity reversal to implement a Loschmidt-echo sequence, thus offering a new powerful tool to perform spectroscopy of strongly correlated samples, to study decoherence phenomena and fidelity in quantum many-body systems [48], and for applications in atom optics. As to the latter, we have demonstrated a novel and efficient atom mirror.

Using the same concept of [18] with phase modulation, we have implemented amplitude modulation to obtain coherent delocalization of atomic wave packets and effectively shorter Bloch-oscillation periods, resulting in sub-ppm sensitivity in the measurement of the local acceleration of gravity. We have discussed conceptual and technical advantages of the present method over previous ones, based on the study of Bloch oscillations either in static or in phase-modulated optical lattices. Allowing the measurement of forces with micrometric spatial resolution and high sensitivity, we can conclude that amplitude modulation provides an excellent tool for the study of potentials at short distances from a surface, e.g. the Casimir–Polder interaction, or for tests of gravitational interaction at micrometric distances [14–19].

Acknowledgments

We thank M Artoni for critical reading, M Schioppo for experimental assistance, V Piazza for helpful discussions and R Ballerini, M De Pas, M Giuntini, A Hajeb, A Montori for technical assistance. This work was supported by LENS, INFN, EU (under contract RII3-CT-2003 506350 and FINAQS), ASI.

References

[1] Bloch I, Dalibard J and Zwerger W 2008 *Rev. Mod. Phys.* **80** 885
[2] Dahan M B, Peik E, Reichel J, Castin Y and Salomon C 1996 *Phys. Rev. Lett.* **76** 4508
[3] Raizen M, Salomon C and Niu Q 1997 *Phys. Today* **50** 30
[4] Greiner M, Mandel O, Esslinger T, Hänsch T W and Bloch I 2002 *Nature* **415** 39
[5] Kinoshita T, Wenger T and Weiss D S 2004 *Science* **305** 1125
[6] Fallani L, Lye J E, Guarrera V, Fort C and Inguscio M 2007 *Phys. Rev. Lett.* **98** 130404
[7] Chin J K, Miller D E, Liu Y, Stan C, Setiawan W, Sanner C, Xu K and Ketterle W 2006 *Nature* **443** 961
[8] Gustavsson M, Haller E, Mark M J, Danzl J G, Rojas-Kopeinig G and Nägerl H C 2008 *Phys. Rev. Lett.* **100** 080404
[9] Fattori M, D'Errico C, Roati G, Zaccanti M, Jona-Lasinio M, Modugno M, Inguscio M and Modugno G 2008 *Phys. Rev. Lett.* **100** 080405
[10] Ludlow A D *et al* 2008 *Science* **319** 1805
[11] Blatt S *et al* 2008 *Phys. Rev. Lett.* **100** 140801
[12] Anderson B P and Kasevich M A 1998 *Science* **282** 1686
[13] Dimopoulos S and Geraci A A 2003 *Phys. Rev.* D **68** 124021
[14] Roati G, de Mirandes E, Ferlaino F, Ott H, Modugno G and Inguscio M 2004 *Phys. Rev. Lett.* **92** 0230402
[15] Carusotto I, Pitaevskii L, Stringari S, Modugno G and Inguscio M 2005 *Phys. Rev. Lett.* **95** 093202
[16] Ferrari G, Poli N, Sorrentino F and Tino G 2006 *Phys. Rev. Lett.* **97** 060402
[17] Wolf P, Lemonde P, Lambrecht A, Bize S, Landragin A and Clairon A 2007 *Phys. Rev.* A **75** 063608
[18] Ivanov V V, Alberti A, Schioppo M, Ferrari G, Artoni M, Chiofalo M L and Tino G M 2008 *Phys. Rev. Lett.* **100** 043602
[19] Müller H, Peters A and Chu S 2010 *Nature* **463** 926
[20] Nelson K D, Li X and Weiss D S 2007 *Nat. Phys.* **3** 556
[21] Anderlini M, Lee P J, Brown B L, Sebby-Strabley J, Phillips W D and Porto J V 2007 *Nature* **448** 452
[22] Bloch I 2008 *Nature* **453** 1016
[23] Mandel O, Greiner M, Widera A, Rom T, Hansch T W and Bloch I 2003 *Phys. Rev. Lett.* **91** 010407
[24] Mandel O, Greiner M, Widera A, Rom T, Hänsch T W and Bloch I 2003 *Nature* **425** 937
[25] Grifoni M and Hänggi P 1998 *Phys. Rep.* **304** 229
[26] Hensinger *et al* 2001 *Nature* **412** 52
[27] Wilkinson S R, Bharucha C F, Madison K W, Niu Q and Raizen M G 1996 *Phys. Rev. Lett.* **76** 4512
[28] Sias C, Lignier H, Singh Y P, Zenesini A, Ciampini D, Morsch O and Arimondo E 2008 *Phys. Rev. Lett.* **100** 040404
[29] Alberti A, Ivanov V V, Tino G M and Ferrari G 2009 *Nat. Phys.* **5** 547
[30] Zenesini A, Lignier H, Ciampini D, Morsch O and Arimondo E 2009 *Phys. Rev. Lett.* **102** 100403
[31] Denschlag J H, Simsarian J E, Häffner H, McKenzie C, Browaeys A, Cho D, Helmerson K, Rolston S and Phillips W D 2002 *J. Phys. B: At. Mod. Opt. Phys.* **35** 3095
[32] Friebel S, D'Andrea C, Walz J, Weitz M and Hänsch T W 1998 *Phys. Rev.* A **57** 20R
[33] Roati G, Jastrzebski W, Simoni A, Modugno G and Inguscio M 2001 *Phys. Rev.* A **63** 052709
[34] Stöferle T, Moritz H, Schori C, Köhl M and Esslinger T 2004 *Phys. Rev. Lett.* **92** 130403
[35] Gell J R *et al* 2008 *Appl. Phys. Lett.* **93** 081115
[36] De Simoni G, Piazza V, Sorba L, Biasiol G and Beltram F 2009 *Appl. Phys. Lett.* **94** 121103
[37] Remeika M, Graves J C, Hammack A T, Meyertholen A D, Fogler M M, Butov L V, Hamron M and Gossard A C 2009 *Phys. Rev. Lett.* **102** 186803
[38] Dunlap D H and Kenkre V M 1986 *Phys. Rev.* B **34** 3625
[39] Thommen Q, Garreau J C and Zehnlé V 2002 *Phys. Rev.* A **65** 053406
[40] Eckardt A, Weiss C and Holthaus M 2005 *Phys. Rev. Lett.* **95** 260404
[41] Drese K and Holthaus M 1997 *Chem. Phys.* **217** 201

[42] Cucchietti F M, Dalvit D A, Paz J P and Zurek W H 2003 *Phys. Rev. Lett.* **91** 210403
[43] Cucchietti F M 2010 *J. Opt. Soc. Am.* B **27** A30
[44] Glück M, Kolovsky A R and Korsch H J 2002 *Phys. Rep.* **366** 103
[45] de Escobar Y N M, Mickelson P G, Pellegrini P, Nagel S B, Traverso A, Yan M, Côté R and Killian T C 2008 *Phys. Rev.* A **78** 062708
[46] Sorrentino F, Alberti A, Ferrari G, Ivanov V V, Poli N, Schioppo M and Tino G M 2009 *Phys. Rev.* A **79** 013409
[47] Harber D M, Obrecht J M, Mcguirk J M and Cornell E A 2005 *Phys. Rev.* A **72** 033610
[48] Zurek W H 2003 *Rev. Mod. Phys.* **75** 715